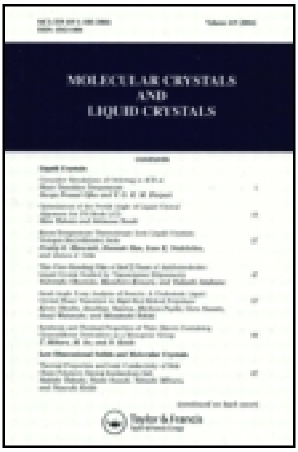

Molecular Crystals and Liquid Crystals Science and Technology. Section A. Molecular Crystals and Liquid Crystals
Publication details, including instructions for authors and subscription information:
http://www.tandfonline.com/loi/gmcl19

Flow Properties of Biaxial Nematic Liquid Crystals

T. Carlsson [a] , F. M. Leslie [b] & J. S. Laverty [b]
[a] Institute of Theoretical Physics, Chalmers University of Technology, S-412 96, Göteborg, Sweden
[b] Department of Mathematics, University of Strathclyde, Livingstone Tower, 26 Richmond Street, Glasgow, G1 1XH, Scotland
Version of record first published: 24 Sep 2006.

Mol. Cryst. Liq. Cryst., 1992, Vol. 210, pp. 95–127
Reprints available directly from the publisher
Photocopying permitted by license only

Printed in the United States of America

Flow Properties of Biaxial Nematic Liquid Crystals

T. CARLSSON
Institute of Theoretical Physics, Chalmers University of Technology, S-412 96 Göteborg, Sweden

and

F. M. LESLIE and J. S. LAVERTY
Department of Mathematics, University of Strathclyde, Livingstone Tower, 26 Richmond Street, Glasgow G1 1XH, Scotland

(Received June 3, 1991)

The equations governing the flow behavior of the biaxial nematic phase are derived and presented in such a form that it is easily seen that the fluid dynamic theory of biaxial nematics can be formulated as a natural generalization of the Leslie-Ericksen theory of uniaxial nematics. It is shown that in order to describe the flow behaviour of biaxial nematics, fifteen viscosity coefficients, related by three Onsager relations, are required. With the biaxial nematic stress tensor as a starting point we discuss the concept of viscous torques, and show how a good qualitative understanding of the flow behaviour of the system follows by studying them. We show that three rotational viscosities and nine effective shearing viscosities have to be defined in order to characterize the viscous behaviour of biaxial nematics completely. Thus it is possible to design sufficient experiments to measure the twelve independent viscosity coefficients included in the theory. We also derive the possible equilibrium orientations for a biaxial nematic when subjected to shear flow, and give a brief discussion of their stability.

Keywords: biaxial nematics, shearing viscosities/biaxial nematics, rotational viscosities/ biaxial nematics, viscosity coefficients/biaxial nematics

I INTRODUCTION

In 1980, Yu and Saupe[1] discovered the existence of a biaxial nematic phase in a multicomponent lyotropic system and more recently thermotropic liquid crystals exhibiting a biaxial nematic phase have also been reported in the literature.[2–4] During the ten years that have passed since the discovery of the biaxial nematic phase, a number of approaches to the description of the fluid dynamics of this system have appeared in the literature.[5–9] Generally, it should be possible to consider the fluid dynamics of biaxial nematics as a generalization of the Leslie-Ericksen theory[10,11] of uniaxial nematics. However, in no instance is the theory of biaxial nematics presented in such a way that this generalization is obvious. A common feature of these theories is that a set of twelve independent viscosity coefficients is necessary in order to describe an isothermal, incompressible biaxial nematic, but in none of the theories is it clear how these coefficients are related to the five independent Leslie coefficients needed to describe the flow behaviour of uniaxial nematics. Furthermore, most of the present theoretical approaches[5–9] to the flow properties of biaxial nematics concentrate on the general mathematical structure of the governing equations of the theory and do not give much consideration to the implications for the physical flow behaviour of the system that can be deduced from these equations.

In this paper we present an alternative formulation of the equations governing the flow behaviour of biaxial nematics, and formulate the theory in such a way that it is easily seen how the fluid dynamic theory of biaxial nematics can be regarded as a natural generalization of the Leslie-Ericksen theory of uniaxial nematics. Thereafter we study the flow properties of the biaxial nematics in detail and show how this behaviour can be viewed as an extension of the corresponding behaviour of uniaxial nematics.

The outline of the paper is as follows: Section II presents a derivation of the governing equations of the fluid dynamics of biaxial nematics, which shows that the symmetry of the system demands in the stress tensor fifteen viscosity coefficients, related by three Onsager relations.

While it is possible to describe a biaxial nematic liquid crystal in several different ways, in Section III we introduce the two directors used in our approach, and show how they are related to the symmetry of the system. Section IV defines the coordinates used in this work, introducing a spherical polar coordinate system which is frequently the most convenient one to use to describe the system.

Section V introduces the concept viscous torque and shows how this can be divided into two parts—the rotational torque connected to rotations of the directors and the shearing torque due to the macroscopic flow of the system. By calculating the expression for the rotational torque, in Section VI we show that three rotational viscosities are necessary to describe the rotational motion of biaxial nematics. Section VII presents a calculation of the shearing torque and derives the equilibrium angles of the directors in shear flow. Section VIII gives a brief discussion of the stability of these equilibrium angles and shows some different examples of flow alignment that can occur in the system.

In Section IX we address the problem of aligning the system by using electric and magnetic fields, and we show that the analysis of the behaviour of the system when subjected to simultaneous electric and magnetic fields is rather involved. However, we are able to show how two crossed electric and magnetic fields can be used to align the two directors.

The problem of determining the full set of viscosity coefficients is discussed in Section X, where we show that it is possible to define nine linearly independent effective shearing viscosities of a biaxial nematic. Thus, together with the three rotational viscosities and the three Onsager relations, there are sufficient relations to permit the full set of viscosity coefficients to be experimentally determined.

Finally, Section XI discusses how the structure of the stress tensor implies that transverse flow can be induced in the system in some cases. By examining the nature of the transverse flow, one can show that the results derived in the previous sections, which are obtained by neglecting the possibility of transverse flow, remain valid.

II THE GOVERNING EQUATIONS—THE BIAXIAL NEMATIC STRESS TENSOR

Here we present a brief account of equations that govern the flow behaviour of a biaxial nematic when surface effects are negligible, so that one ignores the related couple stress arising from the elastic energy. Our aim is to present such theory as a generalization of the corresponding version of the Leslie-Ericksen theory[10,11] for uniaxial nematics. The resulting equations are identical to those given recently by Laverty and Leslie.[12] Whenever possible we employ vector notation, but inevitably in writing tensorial quantities it is necessary to use Cartesian tensor notation.

The anisotropy of a biaxial nematic can be described by two directors $\hat{\mathbf{n}}$ and $\hat{\mathbf{m}}$, and we discuss in the following section a possible interpretation of their roles. For the present it simply suffices to note the constraints arising from their being orthogonal unit vectors,

$$\hat{\mathbf{n}}\cdot\hat{\mathbf{n}} = \hat{\mathbf{m}}\cdot\hat{\mathbf{m}} = 1, \qquad \hat{\mathbf{n}}\cdot\hat{\mathbf{m}} = 0. \tag{II.1}$$

Also adopting the common assumption of incompressibility, the velocity vector $\mathbf{v}$ is subject to the familiar constraint

$$\nabla\cdot\mathrm{v} = 0. \tag{II.2}$$

The relevant balance laws are those expressing conservation of linear and angular momentum,

$$\rho\dot{v}_i = \rho F_i + t_{ij,j} \tag{II.3}$$

and

$$\rho K_i + \varepsilon_{ijk}t_{kj} = 0, \tag{II.4}$$

respectively. In the above ρ denotes density, the superimposed dot a material time derivative, $\mathbf{F}$ and $\mathbf{K}$ body force and body moments per unit mass, respectively, and t_{ij} is the Cauchy stress tensor. In the latter equation the inertial term is omitted, and also the couple stress tensor related to the generalized Frank-Oseen energy.

The body couple arising from a magnetic field $\mathbf{B}$ or an electric field $\mathbf{E}$ is given by

$$\rho K_i = \varepsilon_{ijk}\mathrm{J}_j^b\mathrm{B}_k, \qquad \rho K_i = \varepsilon_{ijk}\mathrm{J}_j^e\mathrm{E}_k, \tag{II.5}$$

where the magnetization $\mathbf{J}^b$ takes the form

$$\mathrm{J}_i^b = \mu_0^{-1}[\chi_n n_i n_j + \chi_m m_i m_j + \chi_l l_i l_j]\mathrm{B}_j, \tag{II.6}$$

and the electric displacement $\mathbf{J}^e$ is given by

$$\mathrm{J}_i^e = \varepsilon_0[\varepsilon_n n_i n_j + \varepsilon_m m_i m_j + \varepsilon_l l_i l_j]\mathrm{E}_j. \tag{II.7}$$

In these equations μ_0 and ε_0 denote the permeability and permittivity of free space, respectively, while χ_i and ε_i are the magnetic susceptibilities and dielectric permittivities, respectively, along the i-axis.

A natural generalization of uniaxial theory assumes that the stress tensor is dependent upon the two directors $\hat{\mathbf{n}}$ and $\hat{\mathbf{m}}$, their material time derivatives $\dot{\hat{\mathbf{n}}}$ and $\dot{\hat{\mathbf{m}}}$, and the velocity gradients $\nabla \mathbf{v}$, being linear in the latter and the time derivatives. With the assumptions of the usual nematic symmetries and invariance requirements, one ultimately obtains

$$\begin{aligned} t_{ij} = {} & \alpha_1 D_{kp} n_k n_p n_i n_j + \alpha_2 N_i n_j + \alpha_3 N_j n_i + \alpha_4 D_{ij} + \alpha_5 D_{ik} n_k n_j \\ & + \alpha_6 D_{jk} n_k n_i + \beta_1 D_{kp} m_k m_p m_i m_j + \beta_2 M_i m_j + \beta_3 M_j m_i \\ & + \beta_5 D_{ik} m_k m_j + \beta_6 D_{jk} m_k m_i + N_p m_p (\mu_1 m_i n_j + \mu_2 n_i m_j) \\ & + D_{kp} n_k m_p (\mu_3 m_i n_j + \mu_4 n_i m_j) - p\delta_{ij} \end{aligned} \tag{II.8}$$

where

$$D_{ij} = \frac{1}{2}(v_{i,j} + v_{j,i}), \qquad W_{ij} = \frac{1}{2}(v_{i,j} - v_{j,i}) \tag{II.9}$$

and

$$N_i = \dot{n}_i - W_{ik} n_k, \qquad M_i = \dot{m}_i - W_{ik} m_k. \tag{II.10}$$

The above form is a relatively straightforward generalization of the expression for a uniaxial nematic[11] except for the omission of two terms, one involving $D_{kp} n_k n_p m_i m_j$ and the other $D_{kp} m_k m_p n_i n_j$. One is omitted on algebraic grounds, it being expressible as a combination of other terms using an argument of the form given by Govers and Vertogen,[13] the other by a stability argument associated with Onsager, which also leads to

$$\alpha_2 + \alpha_3 = \alpha_6 - \alpha_5, \qquad \beta_2 + \beta_3 = \beta_6 - \beta_5, \qquad \mu_1 + \mu_2 = \mu_4 - \mu_3, \tag{II.11}$$

these reducing the number of independent coefficients to twelve.

Finally we note a result required later. Introducing the local angular velocity of the fluid, one can write

$$\dot{\hat{\mathbf{n}}} = \boldsymbol{\omega} \times \hat{\mathbf{n}}, \qquad \dot{\hat{\mathbf{m}}} = \boldsymbol{\omega} \times \hat{\mathbf{m}}. \tag{II.12}$$

From these and the corresponding equation for $\hat{\mathbf{l}}$ where

$$\hat{\mathbf{l}} = \hat{\mathbf{n}} \times \hat{\mathbf{m}}, \tag{II.13}$$

one can show that

$$2\boldsymbol{\omega} = \hat{\mathbf{n}} \times \dot{\hat{\mathbf{n}}} + \hat{\mathbf{m}} \times \dot{\hat{\mathbf{m}}} + \hat{\mathbf{l}} \times \dot{\hat{\mathbf{l}}}, \tag{II.14}$$

a result required in Section VI.

III THE DIRECTORS OF BIAXIAL NEMATICS-CONNECTION BETWEEN THE BIAXIAL AND THE UNIAXIAL NEMATIC VISCOSITY COEFFICIENTS

The microscopic picture that one most often makes of a uniaxial nematic is a rotationally symmetric ellipsoid, the orientational order of which is described by a unit vector $\hat{\mathbf{n}}$, commonly denoted the director (c.f. Figure 1*a*). When studying a biaxial nematic we can refer the biaxiality of the system to the breaking of the rotational symmetry of the ellipsoid around $\hat{\mathbf{n}}$, and instead of studying a system of rotationally symmetric rods we can imagine that we are studying a system consisting of plates with sides of lengths a, b and c for which we assume $a >> b >> c$. To describe such a system one requires two directors. Thus we introduce $\hat{\mathbf{n}}$, the "long director" corresponding to the director of the uniaxial nematic, and $\hat{\mathbf{m}}$, the "transverse director" describing the rotation of the biaxial plate around the long director (c.f. Figure 1*b*). The form of the stress tensor given by Equation (II.8) is readily interpreted in the light of Figure 1. The six α_i-terms, which are those acting on the long director, correspond exactly to the Leslie stress tensor[11] of uniaxial nematics. The five β_i-terms have the same structure as the five anisotropic α_i-terms, only $\hat{\mathbf{n}}$ is replaced by $\hat{\mathbf{m}}$ and thus these terms are acting on the transverse director. We also notice the similarity between the first two of the Onsager relations (II.11) which connect four of the α_i-coefficients and four of the β_i-coefficients, respectively. Finally, there are four μ_i-terms which reflect coupling effects between the long and the transverse directors and which are related by the last of the Onsager relations

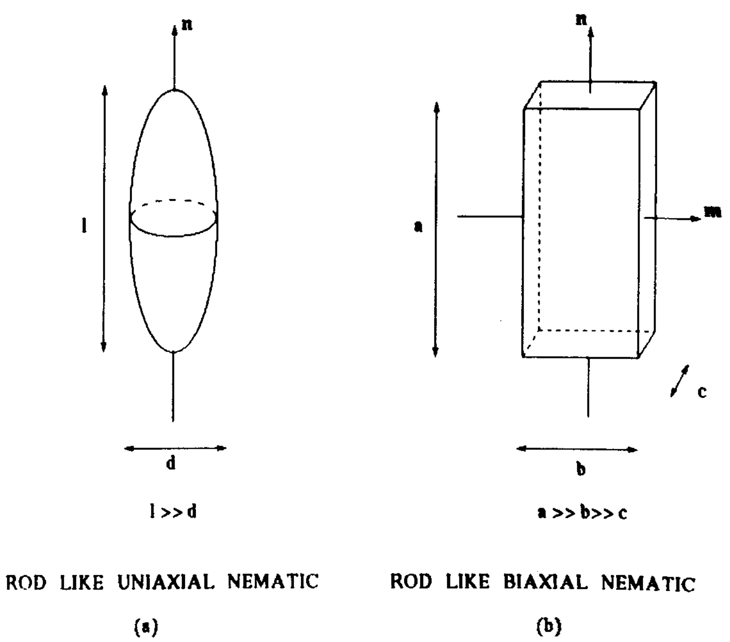

FIGURE 1 Comparison between a rod-like uniaxial nematic (a) and a rod-like biaxial nematic (b). To describe the biaxial nematic, we introduce the biaxial plate. This is completely characterized by specifying the long director $\hat{\mathbf{n}}$ and the transverse director $\hat{\mathbf{m}}$.

(II.11). These terms do not have any counterpart in the Leslie-Ericksen theory of uniaxial nematics.

Above we discuss how the terms of the stress tensor fall into essentially four groups. First of all there is the α_4-term which is the isotropic part of the stress tensor. Then there are the remaining five of the α_i-terms and the five β_i-terms, where the α_i-terms are connected to the n-director in the same way as the β_i-terms are to the m-director. Having restricted ourselves to the study of a biaxial nematic system for which we assume $a >> b >> c$, it is natural to assume that the long director $\hat{\mathbf{n}}$ is more dominant than the transverse director $\hat{\mathbf{m}}$. Thus one expects that the values of the α_i-constants are roughly of the same order as the corresponding Leslie viscosities of a uniaxial nematic, while the β_i-constants are likely to be small compared to their α_i counterpart. Also one expects the β_i-constants to be mutually related to each other in much the same way as the corresponding α_i-constants. Concerning the μ_i-constants, however, we cannot make any firm statement. Being related to the biaxiality of the system, it seems fair to assume that these are small compared to the α_i-constants. In Section V we show that the μ_i-constants cannot be small compared to the β_i-constants.

Finally we point out that the assumption $\alpha_i >> \beta_i$ can be regarded as generally valid for the biaxial nematic with the symmetry pictured in Figure 1*b*. In order to understand this one reasons as follows. First note that one can always assume $\alpha_i > \beta_i$ without loss of generality, because reversing this inequality would simply correspond to interchanging the roles of $\hat{\mathbf{n}}$ and $\hat{\mathbf{m}}$ which is the same as interchanging the lengths a and b. This would simply lead us to study the same physical system by some new coordinates. The case $\alpha_i = \beta_i$ must by symmetry correspond to setting a and b equal and leads us to study a disc like nematic with the director pointing in the direction $\hat{\mathbf{l}} = \hat{\mathbf{n}} \times \hat{\mathbf{m}}$. If $\beta_i \lesssim \alpha_i$ we have a situation which corresponds to a biaxial nematic of the "disc like type," i.e. $a \gtrsim b >> c$. Thus as long as we restrict our study to a biaxial nematic of the "rod like type," i.e., $a >> b >> c$, it seems safe to make the assumptions $\alpha_i >> \beta_i$, $\beta_i \sim \mu_i$ for the viscosity coefficients of the biaxial nematic phase.

IV THE SHEAR FLOW SET UP—DEFINITION OF THE COORDINATES

In order to investigate the flow properties of the biaxial nematic phase we study the system under shear flow, defining the coordinates according to Figure 2. The liquid crystal is confined between two glass plates which are chosen to be parallel to the xy-plane. The lower plate is at rest, while the upper one is moving with the velocity v_0 in the x-direction. In order to describe the two directors, we introduce three angular coordinates in the following way. A spherical polar coordinate system (r, θ, ϕ), of which the angles θ and ϕ are used to describe the long director $\hat{\mathbf{n}}$, is introduced according to Figure 2. Letting the pole of this coordinate system coincide with the z-direction, θ is the angle between the long director and the normal to the plates. We then define ϕ as the angle which the projection of the long director onto the xy-plane makes with the x-axis, counting ϕ positive counter-clockwise. In order to describe the transverse director $\hat{\mathbf{m}}$ we introduce an angle ψ which measures

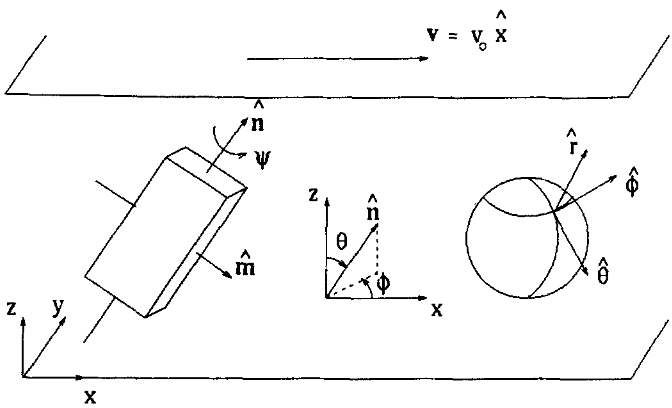

FIGURE 2 Definition of coordinates describing the directors of the biaxial nematic plate. The long director is specified by the polar angles θ and ϕ, while rotation of the transverse director around the long director is given by ψ. In many cases, the quantities we study are most conveniently described by the spherical polar coordinate system (r, θ, ϕ), the base vectors of which are also shown in the figure.

the rotation of the transverse director around the positive $\hat{\mathbf{n}}$-axis. We introduce ψ in such a way that, for each direction of the n-director, $\psi = 0$ corresponds to the transverse director being parallel to $\hat{\phi}$ (c.f. Figure 2 or Equations (IV.2) and (IV.4)). The Cartesian components of the two directors can now be expressed as follows

$$n_x = \sin\theta\cos\phi, \qquad n_y = \sin\theta\sin\phi, \qquad n_z = \cos\theta, \tag{IV.1}$$

and

$$\begin{aligned} m_x &= -\sin\phi\cos\psi - \cos\theta\cos\phi\sin\psi, \\ m_y &= \cos\phi\cos\psi - \cos\theta\sin\phi\sin\psi, \\ m_z &= \sin\theta\sin\psi. \end{aligned} \tag{IV.2}$$

For mathematical convenience, it is at times useful to introduce a third unit vector $\hat{\mathbf{l}} = \hat{\mathbf{n}} \times \hat{\mathbf{m}}$ pointing in the third principal direction of the biaxial plate

$$\begin{aligned} l_x &= -\cos\theta\cos\phi\cos\psi + \sin\phi\sin\psi, \\ l_y &= -\cos\theta\sin\phi\cos\psi - \cos\phi\sin\psi, \\ l_z &= \sin\theta\cos\psi. \end{aligned} \tag{IV.3}$$

The base vectors of the spherical polar coordinate system (r, θ, ϕ) are shown in Figure 2, and can be expressed using Cartesian coordinates as

$$\hat{\mathbf{r}} = \hat{\mathbf{x}}\sin\theta\cos\phi + \hat{\mathbf{y}}\sin\theta\sin\phi + \hat{\mathbf{z}}\cos\theta,$$

$$\hat{\boldsymbol{\theta}} = \hat{\mathbf{x}}\cos\theta\cos\phi + \hat{\mathbf{y}}\cos\theta\sin\phi - \hat{\mathbf{z}}\sin\theta,$$

$$\hat{\boldsymbol{\phi}} = -\hat{\mathbf{x}}\sin\phi + \hat{\mathbf{y}}\cos\phi. \tag{IV.4}$$

Using the spherical coordinate system, one can write $\hat{\mathbf{n}}$, $\hat{\mathbf{m}}$ and $\hat{\mathbf{l}}$ as

$$\hat{\mathbf{n}} = \hat{\mathbf{r}}, \tag{IV.5}$$

$$\hat{\mathbf{m}} = \hat{\boldsymbol{\phi}}\cos\psi - \hat{\boldsymbol{\theta}}\sin\psi, \tag{IV.6}$$

$$\hat{\mathbf{l}} = -\hat{\boldsymbol{\phi}}\sin\psi - \hat{\boldsymbol{\theta}}\cos\psi. \tag{IV.7}$$

From Equations (IV.1) and (IV.2) or (IV.5) and (IV.6) one can easily confirm that the constraints of Equations (II.1) are satisfied.

Assuming that no transverse flow occurs, the velocity field can be written as

$$v_x = v(z), \qquad v_y = 0, \qquad v_z = 0. \tag{IV.8}$$

Thus the local shear flow in this arrangement is everywhere in the x-direction, and for convenience we introduce

$$v' = \frac{dv_x}{dz} \tag{IV.9}$$

as a shorthand notation.

V VISCOUS TORQUES IN BIAXIAL NEMATICS

Neglecting the inertia of the system, the balance law for angular momentum is given by Equation (II.4). The two terms in this equation can be interpreted as the torques which act on the directors due to external and viscous forces, respectively. As external forces we consider only those which are due to electric and magnetic fields, and the corresponding torque ρK_i, which is given by Equations (II.5)–(II.7), is discussed in Section IX. The torque $\varepsilon_{ijk}t_{kj}$ is the viscous torque which we denote by $\mathbf{\Gamma}^v$, and which can be divided into two parts

$$\mathbf{\Gamma}^v = \mathbf{\Gamma}^s + \mathbf{\Gamma}^r = \varepsilon_{ijk}t_{kj} \tag{V.1}$$

Here $\mathbf{\Gamma}^s$ is the shearing torque, i.e., the torque acting on the directors due to the velocity gradient v' while Γ^r is the rotational torque, i.e., the torque which appears if $\dot{\hat{\mathbf{n}}} \neq 0$ or $\dot{\hat{\mathbf{m}}} \neq 0$.

When calculating the torque acting on the directors, one can do so either by using Cartesian coordinates or by using the spherical polar coordinate system introduced by Figure 2. However, if we wish to achieve a good physical interpretation of the torque, as shown below, the spherical polar coordinate system is better suited for the problem than the Cartesian one. Figure 3 pictures the biaxial plate inside the unit sphere, and shows how the torque Γ acting on the system decomposes into its three spherical polar components Γ_r, Γ_θ and Γ_ϕ. Generally, a torque acting on a body causes a rotation around an axis which is parallel to the torque vector. This means that the torque component Γ_r tends to rotate the biaxial plate around the r-axis. Thus this component of the torque causes the transverse director $\hat{\mathbf{m}}$ to rotate around the long director $\hat{\mathbf{n}}$, corresponding to a pure ψ-rotation of the system. In the same way Figure 3 shows that the torque components Γ_θ and Γ_ϕ each act to rotate $\hat{\mathbf{n}}$ in such a way that Γ_θ corresponds to a rotation for which ϕ changes, while Γ_ϕ corresponds to a rotation for which θ changes. This decomposition of the torque into its spherical polar components has been discussed in detail by Carlsson[14] in the case of uniaxial nematics.

VI THE ROTATIONAL TORQUE AND THE ROTATIONAL VISCOSITIES

In this section we derive the expression for the biaxial nematic rotational torque and with this as a starting point define the rotational viscosities of the system. The rotational torque can be expressed as

$$\Gamma_i^r = \varepsilon_{ijk} t_{kj}^r, \tag{VI.1}$$

where t_{kj}^r is the rotational part of the viscous stress tensor, i.e., the part which

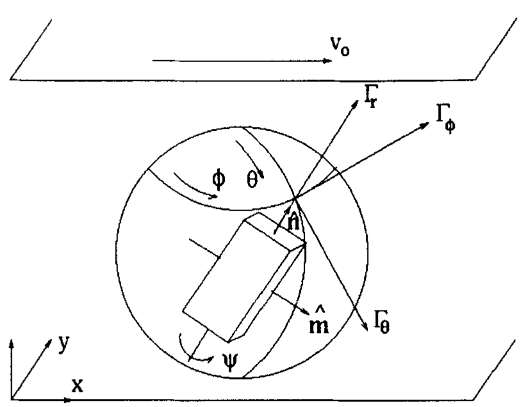

FIGURE 3 The meaning of the spherical polar components of a torque acting on a biaxial nematic. The torque component Γ_r is causing the transverse director $\hat{\mathbf{m}}$ to rotate around the long director $\hat{\mathbf{n}}$, while the torque components Γ_θ and Γ_ϕ each act to rotate the long director $\hat{\mathbf{n}}$ in such a way that Γ_θ corresponds to a rotation for which ϕ changes, while Γ_ϕ corresponds to a rotation for which θ changes.

remains in the absence of velocity gradients. Using Equations (II.8)–(II.10) one obtains

$$t^r_{ij} = \alpha_2 \dot{n}_i n_j + \alpha_3 \dot{n}_j n_i + \beta_2 \dot{m}_i m_j + \beta_3 \dot{m}_j m_i + \dot{n}_p m_p(\mu_1 m_i n_j + \mu_2 n_i m_j). \quad \text{(VI.2)}$$

The calculation is most easily performed using spherical polar coordinates, and to do so we first calculate the time derivatives of the corresponding base vectors which are given by Equations (IV.4).

$$\begin{aligned} \dot{\hat{\mathbf{r}}} &= \dot{\theta}\,\hat{\theta} + \dot{\phi}\sin\theta\,\hat{\phi}, \\ \dot{\hat{\theta}} &= -\dot{\theta}\,\hat{\mathbf{r}} + \dot{\phi}\cos\theta\,\hat{\phi}, \\ \dot{\hat{\phi}} &= -\dot{\phi}\sin\theta\,\hat{\mathbf{r}} - \dot{\phi}\cos\theta\,\hat{\theta}. \end{aligned} \quad \text{(VI.3)}$$

From Equations (IV.5), (IV.6) and (VI.3) one can now derive expressions for the time derivatives of the directors

$$\dot{\mathbf{n}} = \dot{\theta}\,\hat{\theta} + \dot{\phi}\sin\theta\,\hat{\phi}, \quad \text{(VI.4)}$$

$$\begin{aligned} \dot{\mathbf{m}} &= \hat{\mathbf{r}}(\dot{\theta}\sin\psi - \dot{\phi}\sin\theta\cos\psi) - \hat{\theta}\cos\psi(\dot{\phi}\cos\theta + \dot{\psi}) \\ &\quad - \hat{\phi}\sin\psi(\dot{\phi}\cos\theta + \dot{\psi}). \end{aligned} \quad \text{(VI.5)}$$

Also one finds the time derivative of $\hat{\mathbf{l}}$ to be

$$\begin{aligned} \dot{\hat{\mathbf{l}}} &= \hat{\mathbf{r}}(\dot{\theta}\cos\psi + \dot{\phi}\sin\theta\sin\psi) + \hat{\theta}\sin\psi(\dot{\phi}\cos\theta + \dot{\psi}) \\ &\quad - \hat{\phi}\cos\psi(\dot{\phi}\cos\theta + \dot{\psi}). \end{aligned} \quad \text{(VI.6)}$$

At this stage it is possible to calculate the angular velocity $\boldsymbol{\omega}$ (Equation (II.14)) of the biaxial plate, a quantity which will prove useful later,

$$\boldsymbol{\omega} = \hat{\mathbf{r}}(\dot{\phi}\cos\theta + \dot{\psi}) - \hat{\theta}\,\dot{\phi}\sin\theta + \hat{\phi}\,\dot{\theta}. \quad \text{(VI.7)}$$

From Equations (VI.2), (VI.4) and (VI.5) one can calculate the components of the rotational stress tensor and by the use of Equation (VI.1) the spherical polar components of the rotational torque turn out to be

$$\begin{aligned} \Gamma^r_r &= -(\beta_3 - \beta_2)(\dot{\phi}\cos\theta + \dot{\psi}), \\ \Gamma^r_\theta &= (\alpha_3 - \alpha_2)\dot{\phi}\sin\theta \\ &\quad + (\beta_3 - \beta_2 + \mu_2 - \mu_1)(\dot{\phi}\sin\theta\cos^2\psi - \dot{\theta}\sin\psi\cos\psi), \\ \Gamma^r_\phi &= -(\alpha_3 - \alpha_2)\dot{\theta} \\ &\quad - (\beta_3 - \beta_2 + \mu_2 - \mu_1)(\dot{\theta}\sin^2\psi - \dot{\phi}\sin\theta\sin\psi\cos\psi). \end{aligned} \quad \text{(VI.8)}$$

Generally, the rotational torque is related to the angular velocity of the system through a rotational viscosity tensor $\boldsymbol{\gamma}^r$ by the relation

$$\boldsymbol{\Gamma}^r = -\boldsymbol{\gamma}^r\boldsymbol{\omega}. \tag{VI.9}$$

An inspection of Equations (VI.7)–(VI.9) shows that the rotational viscosity tensor is

$$\boldsymbol{\gamma}^r = \begin{pmatrix} \beta_3 - \beta_2 & 0 & 0 \\ 0 & \alpha_3 - \alpha_2 + (\beta_3 - \beta_2 + \mu_2 - \mu_1)\cos^2\psi & (\beta_3 - \beta_2 + \mu_2 - \mu_1)\sin\psi\cos\psi \\ 0 & (\beta_3 - \beta_2 + \mu_2 - \mu_1)\sin\psi\cos\psi & \alpha_3 - \alpha_2 + (\beta_3 - \beta_2 + \mu_2 - \mu_1)\sin^2\psi \end{pmatrix} \tag{VI.10}$$

Demanding $\boldsymbol{\gamma}^r$ to be positive definite leads to the following three conditions

$$\gamma_n = \alpha_3 - \alpha_2 > 0,$$

$$\gamma_m = \beta_3 - \beta_2 > 0,$$

$$\gamma_{nm} = \alpha_3 - \alpha_2 + \beta_3 - \beta_2 + \mu_2 - \mu_1 > 0. \tag{VI.11}$$

In Equations (VI.11) we have introduced the notations γ_n, γ_m and γ_{nm}. Each of these quantities is related to the rotation of the biaxial plate around one of its three principal axes and is what we term a rotational viscosity of the system. Figure 4 shows the corresponding rotations of the biaxial plate. In Figure 4*a* the transverse

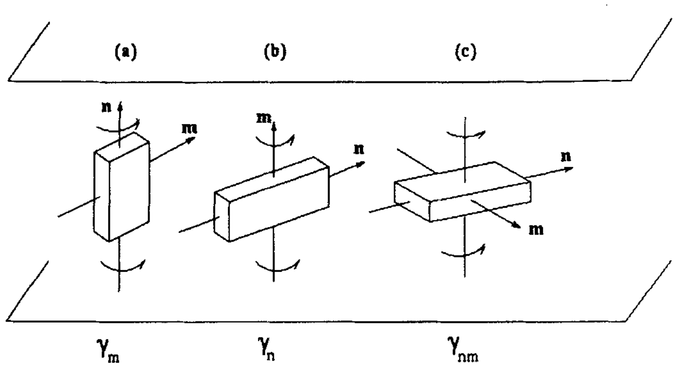

FIGURE 4 Definition of the three rotational viscosities of a biaxial nematic.

director $\hat{\mathbf{m}}$ rotates around the long director $\hat{\mathbf{n}}$. The corresponding rotational viscosity can be deduced by putting $\theta = \phi = 0$ in Equations (VI.8) to give

$$\boldsymbol{\Gamma}^r = -(\beta_3 - \beta_2)\dot{\psi}\,\hat{\mathbf{r}} = -\gamma_m\dot{\psi}\hat{\mathbf{r}}. \quad \text{(VI.12)}$$

In Figure 4*b* the long director $\hat{\mathbf{n}}$ rotates around the transverse director $\hat{\mathbf{m}}$. This situation is achieved by putting $\phi = \psi = 0$ in Equations (VI.8) leading to

$$\boldsymbol{\Gamma}^r = -(\alpha_3 - \alpha_2)\dot{\theta}\hat{\phi} = -\gamma_n\dot{\theta}\hat{\phi}. \quad \text{(VI.13)}$$

The two rotational viscosities γ_n and γ_m thus correspond to the situations for which only one of the two directors rotates, and their structure confirms the conclusion in Section III that the β_i-coefficients are related to the m-director in the same way as the α_i-coefficients are to the n-director. Finally, in Figure 4*c* we show the situation in which both the directors are rotating around the l-axis. This is achieved by putting $\phi = 0$, $\psi = \pi/2$ and in this case Equations (VI.8) give the rotational torque

$$\boldsymbol{\Gamma}^r = -(\alpha_3 - \alpha_2 + \beta_3 - \beta_2 + \mu_2 - \mu_1)\dot{\theta}\hat{\phi} = -\gamma_{nm}\dot{\theta}\hat{\phi}. \quad \text{(VI.14)}$$

Here we note that the corresponding rotational viscosity is not just the sum of the two rotational viscosities corresponding to the two directors rotating separately, but instead takes the form

$$\gamma_{nm} = \gamma_n + \gamma_m + \mu_2 - \mu_1 \quad \text{(VI.15)}$$

where the term $\mu_2 - \mu_1$ represents a nonlinear coupling between the rotations of the two directors.

While the three inequalities (VI.11) must always hold on thermodynamic grounds, we now write down another inequality, which seems plausible by the following reasoning. As a much larger surface of the biaxial plate has to trace its way through the liquid in the case of Figure 4*b* compared to that of Figure 4*c*, it is obvious that we should expect the rotational viscosity γ_n to be larger than that of γ_{nm}. This leads to the inequality

$$\mu_1 - \mu_2 > \beta_3 - \beta_2. \quad \text{(VI.16)}$$

From Equations (VI.11), $\beta_3 - \beta_2$ is always positive, and as a consequence it follows from Equation (VI.16) that the inequality

$$\mu_1 > \mu_2 \quad \text{(VI.17)}$$

must always be fulfilled by the two coupling coefficients μ_1 and μ_2.

The form of the rotational torque as given by Equations (VI.8) implies an interesting cross effect in the rotational behavior of the system. In Figure 5 we show the rotation of the biaxial plate in the case when the long director $\hat{\mathbf{n}}$ is confined

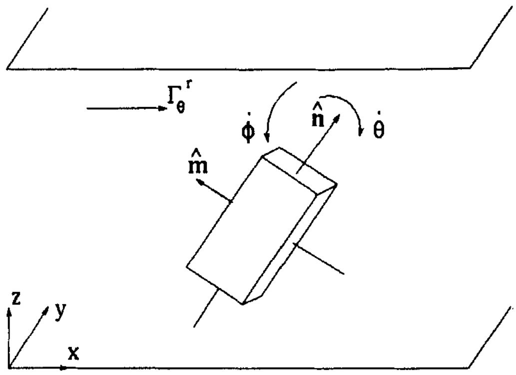

FIGURE 5 Demonstration of transverse torque effects in the rotational motion of a biaxial nematic. In the figure, the long director $\hat{\mathbf{n}}$ is confined within the xz-plane performing a rotation $\dot\theta \neq 0$. If the transverse director $\hat{\mathbf{m}}$ makes an oblique angle with the xz-plane, a transverse torque Γ_θ^r is exerted on the long director, causing it to rotate out of this plane.

within the shearing plane, while the transverse director $\hat{\mathbf{m}}$ makes an oblique angle with the shear plane. This corresponds to $\phi = 0$, $\psi \neq 0$, $\pi/2$ and $\dot\theta \neq 0$. Apart from the expected counteracting torque Γ_ϕ^r, there will also be a transverse torque component Γ_θ^r given by

$$\Gamma_\theta^r = -(\beta_3 - \beta_2 + \mu_2 - \mu_1)\dot\theta\sin\psi\cos\psi. \qquad \text{(VI.18)}$$

In the same way it is easy to convince oneself that whenever the long director is rotating around an axis which does not coincide with one of the other two principal axes of the biaxial plate, such a transverse torque always appears. This fact makes the analysis of the routes towards equilibrium in many cases much more complex than one might have imagined at first. Let us further assume that the x-component of $\hat{\mathbf{m}}$ is negative (i.e., $0 < \psi < \pi/2$) as pictured in Figure 5. By physical reasoning, we then expect the transverse torque acting on the long director to rotate it in the negative ϕ-direction. This corresponds to, as can be seen from Figures 2 and 3, a positive torque Γ_θ^r. Demanding Γ_θ^r given by Equation (VI.18) to be positive rederives the inequality (VI.16) arrived at above by completely different reasoning. Thus, even if this inequality is not a strict inequality in the thermodynamic sense, it seems to us safe to introduce it as a consequence of the geometry of the particular system we are modeling.

Finally we clarify that if the long director is rotating at constant θ, i.e., is tracing out a cone around the z-axis, the reference direction for which $\psi = 0$ rotates also. This is the origin of the term $\dot\phi\cos\theta$ in the expression for Γ_γ^r in the first of Equations (VI.8). If such a rotation is performed keeping $\hat{\mathbf{m}}$ constant, i.e., for zero torque Γ_γ^r, ψ must all the time change according to $\dot\psi = -\dot\phi\cos\theta$ because of the rotation of the reference direction of ψ.

VII THE SHEARING TORQUE AND THE FLOW ALIGNMENT ANGLES

We now calculate the shearing torque acting on the biaxial plate using the coordinates introduced in Figure 2. In absence of transverse flow, the velocity field is given by Equation (IV.8) and thus the only nonzero components of the strain rate and vorticity tensors (Equations (II.9) are

$$D_{xz} = D_{zx} = \frac{1}{2} v', \tag{VII.1}$$

$$W_{xz} = -W_{zx} = \frac{1}{2} v'. \tag{VII.2}$$

The two vectors N_i and M_i become in the case of a steady shear flow (i.e., $\dot{n}_i = \dot{m}_i = 0$)

$$N_x^s = -\frac{1}{2} v' n_z,$$

$$N_y^s = 0,$$

$$N_z^s = \frac{1}{2} v' n_x, \tag{VII.3}$$

and

$$M_x^s = -\frac{1}{2} v' m_z,$$

$$M_y^s = 0,$$

$$M_z^s = \frac{1}{2} v' m_x. \tag{VII.4}$$

The Cartesian components of the shearing torque calculated from Equations (II.8), (V.1) and (VII.1)–(VII.4) take the form

$$\Gamma_x^s = v'[-\alpha_3 n_x n_y - \beta_3 m_x m_y + (n_z m_y - n_y m_z)(\mu_1 n_z m_x + \mu_2 n_x m_z)],$$

$$\Gamma_y^s = v'[-\alpha_2 n_z^2 + \alpha_3 n_x^2 - \beta_2 m_z^2 + \beta_3 m_x^2 + (n_x m_z - n_z m_x)(\mu_1 n_z m_x + \mu_2 n_x m_z)] \tag{VII.5}$$

$$\Gamma_z^s = v'[\alpha_2 n_y n_z + \beta_2 m_y m_z + (n_y m_x - n_x m_y)(\mu_1 n_z m_x + \mu_2 n_x m_z)].$$

As was explained in Section V, we prefer to express the torque by the use of the spherical polar coordinate system introduced in Figures 2 and 3. Introducing the coordinates of n_i and m_i as given by Equations (IV.1) and (IV.2) and the expressions for the base vectors $\hat{\mathbf{r}}$, $\hat{\theta}$ and $\hat{\phi}$ (Equations (IV.4)), we can now calculate the projections of the torque (VII.5) into the r-, θ- and ϕ-directions, to give

$$\begin{aligned}
\Gamma_r^s &= v'[\beta_3(\sin\theta\sin\phi\cos^2\psi + \sin\theta\cos\theta\cos\phi\sin\psi\cos\psi) \\
&\quad + \beta_2(\sin\theta\cos\theta\cos\phi\sin\psi\cos\psi - \sin\theta\sin\phi\sin^2\psi)], \\
\Gamma_\theta^s &= v'[-\alpha_2\cos\theta\sin\phi - \beta_2\sin^2\theta\cos\phi\sin\psi\cos\psi \\
&\quad + \beta_3(\cos\theta\sin\phi\cos^2\psi + \cos^2\theta\cos\phi\sin\psi\cos\psi) \\
&\quad - \mu_1\cos\theta\sin\phi\cos^2\psi + \cos\phi\sin\psi\cos\psi(\mu_2\sin^2\theta - \mu_1\cos^2\theta)], \\
\Gamma_\phi^s &= v'[(\alpha_3\sin^2\theta - \alpha_2\cos^2\theta)\cos\phi - \beta_2\sin^2\theta\cos\phi\sin^2\psi \\
&\quad + \beta_3(\cos\theta\sin\phi\sin\psi\cos\psi + \cos^2\theta\cos\phi\sin^2\psi) \\
&\quad - \mu_1\cos\theta\sin\phi\sin\psi\cos\psi + \cos\phi\sin^2\psi(\mu_2\sin^2\theta - \mu_1\cos^2\theta)].
\end{aligned} \tag{VII.6}$$

In order to start to understand how the shearing torque of Equations (VII.6) influences the biaxial plate, we investigate a few special cases. In Figure 6, the six different flows achievable by letting the three principal axes of the biaxial plate fall along the x-, y- and z-axes are shown. In all of these cases, the torque acting on the plate is parallel to the y-axis. In Figure 6*a* we have chosen the situation for which $\hat{\mathbf{m}}$ is parallel to $\hat{\mathbf{y}}$. The torque acting on the system in this case acts solely on the long director and is given by $\mathbf{\Gamma}^s = -\alpha_2 v'\hat{\mathbf{y}}$ or $\mathbf{\Gamma}^s = \alpha_3 v'\hat{\mathbf{y}}$, depending on whether the long director is perpendicular to the plates or parallel to the direction of the flow. In this case, the m-director is pointing in the isotropic direction and the system behaves just as a uniaxial nematic would do in the same situation.[11,14] In Figure 6*b*, instead the n-director is pointing in the isotropic direction. The torque in this case again points in the y-direction and thus acts only to rotate the transverse director, being $\mathbf{\Gamma}^s = -\beta_2 v'\hat{\mathbf{y}}$ and $\mathbf{\Gamma}^s = \beta_3 v'\hat{\mathbf{y}}$, respectively. We notice that in the latter case, we have simply replaced α_i by β_i, again confirming that in the two cases discussed above, the β_i-coefficients are connected to the m-director in just the same way as the α_i-coefficients are to the n-director. The case when both the directors are confined in the shearing plane is shown in Figure 6*c*. Here the torques in the two situations are given by $\mathbf{\Gamma}^s = (-\alpha_2 + \beta_3 - \mu_1)v'\hat{\mathbf{y}}$ and $\mathbf{\Gamma}^s = (\alpha_3 - \beta_2 + \mu_2)v'\hat{\mathbf{y}}$, respectively. Thus we notice that one cannot merely add the torques acting on the two directors as they are given by Figures 6*a* and *b*, but that there is also a contribution to the torque from the coupling terms connected to μ_1 and μ_2.

In order to determine the possible equilibrium angles of the directors one must assign values to the viscosity coefficients which appear in the expressions for the

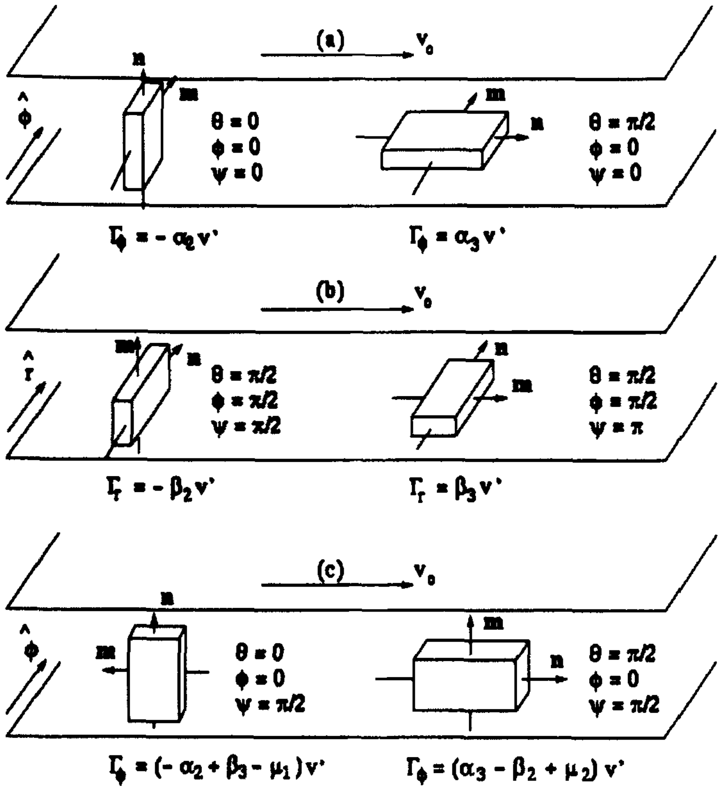

FIGURE 6 Shearing torques acting on the biaxial plate when its three principal axes coincide with the x-, y- and z-axes.

TABLE I

Inequalities restricting the values of the six viscosity coefficients entering the expression of the viscous torque of a rod-like biaxial nematic

$\alpha_2 < 0$	$\beta_2 < 0$	Must be fulfilled
$\alpha_3 < 0$ $\lvert\alpha_2\rvert >> \lvert\alpha_3\rvert$	$\beta_3 < 0$ $\lvert\beta_2\rvert >> \lvert\beta_3\rvert$	Most probable possibility Plausible relation in this case
$\alpha_3 > 0$	$\beta_3 > 0$	Possible but probably rare situation
$\alpha_3 - \alpha_2 > 0$ $\alpha_3 - \alpha_2 + \beta_3 - \beta_2 + \mu_2 - \mu_1 > 0$	$\beta_3 - \beta_2 > 0$	Must always be fulfilled
$\mu_1 - \mu_2 > \beta_3 - \beta_2$ $\mu_1 > \mu_2$		Must be fulfilled for a "rod-like" biaxial nematic

shearing torque. As no experimental information concerning these constants is presently available, we try to make a sound guess as to their qualitative values and, what is even more important, their signs. As the α_i-coefficients correspond to the Leslie coefficients of a uniaxial nematic it seems reasonable to assume that they are also of the same order[15,16] in the biaxial case. Thus, for the rod-like biaxial nematic which we are modeling, one assumes α_2 to be negative, while α_3 should most commonly be negative fulfilling the relation $|\alpha_3| << |\alpha_2|$. We cannot, however, exclude the possibility that α_3 is positive. Furthermore, while it is reasonable to assume that the values of the β_i-coefficients behave like those of the α_i, we generally assume $\beta_i << \alpha_i$ as a consequence of the fact that the β_i-coefficients represent the biaxiality regarded as a small disturbance to the uniaxiality of the system. We thus assume $\beta_2 < 0$, while allowing β_3 to be positive as well as negative, probably with $\beta_3 < 0$ the more common situation. In this latter case, it seems reasonable to assume the relation $|\beta_3| << |\beta_2|$ to be valid. Concerning the coefficients μ_1 and μ_2 we believe their magnitude to be small compared to $|\alpha_2|$. However, they cannot be neglected compared to the β_i-constants because of the inequality (VI.16). Also from the inequality (VI.17), one must always demand $\mu_1 > \mu_2$. In Table I we have summarized our view of the six viscosity coefficients which enter the expressions of the viscous torque of the system.

Going back to Figure 6, one sees that, with our assumptions for the viscosity coefficients, for all the three configurations in the left hand column of the figure the torque acting on the biaxial plate is pointing along the positive y-axis, thus tending to rotate the plate clockwise. Studying the three configurations in the right hand column of the figure, it is clear that the torque acts along the negative y-axis provided that α_3, β_3 and $\alpha_3 - \beta_2 + \mu_2$ are all negative, respectively. In these cases one expects that the system could find an equilibrium for some intermediate inclination of the plate between these of the left hand and the right hand columns. To find the possible equilibrium configurations of the system under shear, one returns to Equations (VII.6) and determines the angles for which $\mathbf{\Gamma}^s = 0$. Under the assumptions that α_2, β_2 and $\alpha_2 - \beta_3 + \mu_1$ as well as α_3, β_3 and $\alpha_2 - \beta_3 + \mu_1$ are all negative there are six solutions, all appearing in pairs. These six solutions are shown in Figure 7.

For the solution shown in Figure 7*a* the m-director is pointing in the y-direction, while the n-director is confined within the shearing plane. The corresponding equilibrium angles are given by

$$\textbf{FP} \quad \phi = \psi = 0, \qquad \cos 2\theta = \frac{\alpha_3 - \alpha_2}{\alpha_3 + \alpha_2} \tag{VII.7}$$

$$\textbf{BP} \quad \phi = \pi, \qquad \psi = 0, \qquad \cos 2\theta = \frac{\alpha_3 - \alpha_2}{\alpha_3 + \alpha_2} \tag{VII.8}$$

We introduce the shorthand notation **FP** and **BP** for these two solutions. This notation is to be interpreted in such a way that the first letter refers to the long director pointing in the forward and backward direction, respectively, while the second letter indicates that the transverse director is pointing in the perpendicular direction.

For the solutions in Figure 7*b* the long director is pointing in the y-direction.

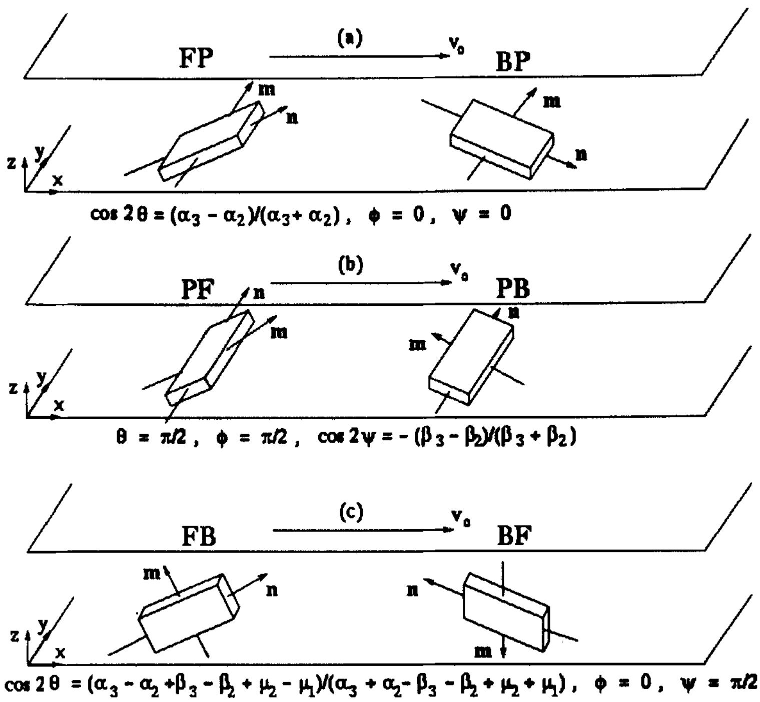

FIGURE 7 Equilibrium orientations of the biaxial plate when subjected to shear flow. In order to distinguish the different solutions we have introduced the shorthand notation shown in the figure. This is to be interpreted in such a way that the first letter refers to the long director pointing in the forward, backward or perpendicular direction, respectively. In the same way the second letter refers to the direction of the transverse director.

We then find the two possible equilibrium angles for the m-director in the shearing plane to be given by

$$\textbf{PF} \quad \theta = \phi = \pi/2, \quad \cos 2\psi = -\frac{\beta_3 - \beta_2}{\beta_3 + \beta_2}, \quad \sin 2\psi < 0 \qquad \text{(VII.9)}$$

$$\textbf{PB} \quad \theta = \phi = \pi/2, \quad \cos 2\psi = -\frac{\beta_3 - \beta_2}{\beta_3 + \beta_2}, \quad \sin 2\psi > 0 \qquad \text{(VII.10)}$$

These two solutions are denoted by **PF** and **PB**, respectively, meaning that the long director is pointing in the perpendicular direction, while the transverse director is pointing in the forward and backward direction, respectively. To appreciate the similarity between the solutions (VII.7), (VII.8) and (VII.9), (VII.10) one observes that the minus sign in Equations (VII.9) and (VII.10) is due to the fact that the reference directions for θ and ψ in the two cases are not the same. From Figures 7*a* and *b* we thus see that the possible flow alignment for the two directors is similar to that most often occurring in uniaxial nematic systems.

Finally, for the two solutions shown in Figure 7*c* both the directors are confined within the shearing plane. Here we again have two equilibrium angles given by

$$\textbf{FB} \quad \phi = 0, \psi = \pi/2, \quad \cos 2\theta = \frac{\alpha_3 - \alpha_2 + \beta_3 - \beta_2 + \mu_2 - \mu_1}{\alpha_3 + \alpha_2 - \beta_3 - \beta_2 + \mu_2 + \mu_1} \quad \text{(VII.11)}$$

$$\textbf{BF} \quad \phi = \pi, \psi = \pi/2, \quad \cos 2\theta = \frac{\alpha_3 - \alpha_2 + \beta_3 - \beta_2 + \mu_2 - \mu_1}{\alpha_3 + \alpha_2 - \beta_3 - \beta_2 + \mu_2 + \mu_1} \quad \text{(VII.12)}$$

which we denote **FB** and **BF**, respectively. Again note that due to the coupling, the torques acting on the n- and m-directors do not simply add up, but the expression for $\cos 2\theta$ also involves the coupling coefficients μ_1 and μ_2.

The six equilibrium configurations pictured in Figure 7 are obtained if the assumptions concerning the viscous coefficients discussed above are fulfilled. Naturally there is no reason to prohibit the coefficients α_3 or β_3 from taking positive values, even if this probably is a rare situation. Thus any pair of the solutions given by Equations (VII.7)–(VII.12) might not exist, and we can expect situations where there are either zero, two, four or six equilibrium orientations of the biaxial plate.

Finally, a few words about the stability of the equilibrium configurations which are shown in Figure 7. In order to investigate the stability of these, we must calculate the torque corresponding to all possible infinitesimal perturbations to the solutions. If the torque always tends to take the system back towards the original solution the equilibrium is stable. As we are working in a three-dimensional space, there are a vast number of possibilities for the nature of the singular points of the torque pattern. We also have a large number of parameters that can be varied rather independently. A complete understanding of the stability properties of the possible solutions would demand a tedious investigation. Such an investigation is in progress.[17] In the next section, however, we limit ourselves to discuss just a few different examples of stability that can be exhibited by the system.

VIII STABILITY OF THE FLOW EQUILIBRIUM ANGLES—EXISTENCE OF FLOW ALIGNMENT

As was shown in the previous section, there are six different orientations of the biaxial plate for which the shearing torque vanishes (c.f. Figure 7). In this section we discuss how the stability of these configurations depends upon the viscosity coefficients of the system. It is easy to convince oneself that any pair of the solutions (VII.7)–(VII.12) may or may not exist independently from each other. With the assumptions $\alpha_2 < 0$, $\beta_2 < 0$ and α_2 having the largest magnitude of all the viscosity coefficients, the condition for the existence of each pair of the solution reads

$$\textbf{FP and BP} \quad \alpha_3 < 0, \quad \text{(VIII.1)}$$

$$\textbf{PF and PB} \quad \beta_3 < 0, \quad \text{(VIII.2)}$$

$$\textbf{FB and BF} \quad \alpha_3 - \beta_2 + \mu_2 < 0. \quad \text{(VIII.3)}$$

In order to achieve a qualitative understanding of the behaviour of the system in shear flow, one must now determine the stability of the flow equilibrium angles. A complete understanding of this problem demands a rather extensive investigation and will be presented in future work.[17] Here we simply give a brief discussion of the problem and show a few different examples of the stability properties of the system. The starting point for this investigation is the torque equation

$$\mathbf{\Gamma}^r + \mathbf{\Gamma}^s = 0 \tag{VIII.4}$$

where $\mathbf{\Gamma}^r$ and $\mathbf{\Gamma}^s$ are given by Equations (VI.8) and (VII.6), respectively. Equation (VIII.4) represents the governing equations of a dynamical system and has the structure

$$\begin{aligned} \dot{\theta} &= f_1(\theta, \phi, \psi), \\ \dot{\phi} &= f_2(\theta, \phi, \psi), \\ \dot{\psi} &= f_3(\theta, \phi, \psi). \end{aligned} \tag{VIII.5}$$

The flow equilibrium angles represent the stationary points of the dynamical system (VIII.5), i.e., the points for which $f_1 = f_2 = f_3 = 0$. To determine the stability of a solution $\theta = \theta_0$, $\phi = \phi_0$ and $\psi = \psi_0$ we introduce three perturbation angles α, β and γ according to

$$\begin{aligned} \theta &= \theta_0 + \alpha, \\ \phi &= \phi_0 + \beta, \\ \psi &= \psi_0 + \gamma. \end{aligned} \tag{VIII.6}$$

Expanding Equations (VIII.5) to linear order in these perturbations gives

$$\begin{aligned} \dot{\alpha} &= \alpha_{11}\alpha + \alpha_{12}\beta + \alpha_{13}\gamma, \\ \dot{\beta} &= \alpha_{21}\alpha + \alpha_{22}\beta + \alpha_{23}\gamma, \\ \dot{\gamma} &= \alpha_{31}\alpha + \alpha_{32}\beta + \alpha_{33}\gamma. \end{aligned} \tag{VIII.7}$$

A nice introduction to the analysis of such a dynamical system is given in a book by Meirovitch.[18] Following Meirovitch, the nature of the equilibrium points is now determined by the eigenvalues of the matrix α_{ij}. If all the three eigenvalues are real and negative, the equilibrium is stable and is denoted a stable node (SN). If one eigenvalue is negative and the other two are complex conjugates with a negative real part, the equilibrium is still stable, but is denoted a stable focus (SF). If at least one of the eigenvalues is positive or has a positive real part, the equilibrium is unstable. Some types of unstable equilibrium points are the unstable node (UN) for which all three eigenvalues are positive, the saddle point (SP) for which the eigenvalues are real and of different signs and the unstable focus (UF) for which two eigenvalues are complex conjugates with a positive real part.

To perform a full survey of the stability properties of the equilibrium points of the system would lead too far to be carried through here. Such an investigation will be presented by us elsewhere.[17] Here we are content to give a few examples of different types of stability which might occur in the system. In Table II, we show the outcome of a stability analysis for six different sets of viscosity coefficients. From this we see that it is possible to find parameter values for which each one of the three solutions **FP**, **FB** and **PF** is stable. We did not find any set of viscosity coefficients for which more than one of these three equilibrium points were stable at the same time, but presently we cannot rule out this possibility. It is, however, easy to see that the three solutions **BP**, **BF** and **PB** cannot be stable if the assumptions $\alpha_2 < 0$, $\beta_2 < 0$ and $|\alpha_2| > |\beta_2|, |\mu_1 + \mu_2|$ are valid. Situations for which none of the present solutions is stable do also exist. The choice of the values of the viscosity coefficients used for the analysis presented in Table II is made to fulfill the conditions which are displayed in Table I. At the present stage, however, it is hard to decide how realistic the parameter values used are, and it is thus difficult to state which of the situations displayed in Table II are realizable in a real biaxial nematic system.

IX INTERACTION WITH ELECTRIC AND MAGNETIC FIELDS

We now discuss the orientational effects on the biaxial plate that appear in the presence of electric and/or magnetic fields over the sample. In order to describe the dielectric and magnetic properties of the medium we have to introduce three dielectric permittivities and three magnetic susceptibilities, one for each principal axis of the biaxial plate. We denote these six constants ε_i and χ_i, respectively, where ε_i corresponds to the dielectric permittivity along the i-axis and so on (c.f. Figure 8). Instead of discussing the problem in terms of the susceptibilities intro-

TABLE II

A selection of possible equilibrium situations for a biaxial nematic under shear. In the table the solutions which are stable, thus referring to a flow alignment, are printed in bold

Parameter Values						Solution and Stability		
α_2	α_3	β_2	β_3	μ_1	μ_2	**FP BP**	**FB BF**	**PF PB**
-10^{-1}	-10^{-2}	-10^{-3}	-10^{-4}	$+2\cdot10^{-2}$	$-5\cdot10^{-2}$	**SN** UN	SP SP	SP SP
-10^{-1}	-10^{-3}	-10^{-3}	-10^{-4}	$+2\cdot10^{-2}$	$-5\cdot10^{-2}$	**SF** UF	SP SP	SP SP
-10^{-1}	-10^{-2}	-10^{-3}	$+2\cdot10^{-3}$	$+4\cdot10^{-3}$	-10^{-3}	SP SP	**SN** UN	— —
-10^{-1}	-10^{-2}	-10^{-3}	$+2\cdot10^{-3}$	$+7\cdot10^{-2}$	-10^{-2}	SP SP	**SF** UF	— —
-10^{-1}	-10^{-5}	-10^{-3}	-10^{-4}	$+4.4\cdot10^{-2}$	$+4\cdot10^{-2}$	SP SP	— —	**SF** UF
-10^{-1}	$-5\cdot10^{-3}$	-10^{-3}	-10^{-4}	$+4.4\cdot10^{-2}$	$+4\cdot10^{-2}$	SP SP	— —	SP SP

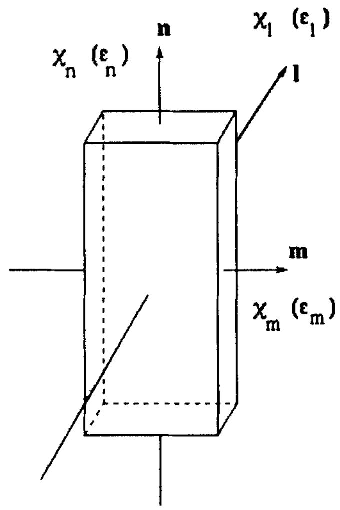

FIGURE 8 Definition of the magnetic susceptibilities χ_i and the dielectric permittivities ε_i of the biaxial plate.

duced above, it is sometimes more convenient to introduce the corresponding dielectric and magnetic anisotropies,

$$\varepsilon_{nm} = \varepsilon_n - \varepsilon_m, \qquad \varepsilon_{nl} = \varepsilon_n - \varepsilon_l, \qquad \varepsilon_{ml} = \varepsilon_m - \varepsilon_l,$$

$$\chi_{nm} = \chi_n - \chi_m, \qquad \chi_{nl} = \chi_n - \chi_l, \qquad \chi_{ml} = \chi_m - \chi_l. \tag{IX.1}$$

When applying a magnetic field **B** over the system, there is an induced magnetization $\mathbf{J}^b$ according to

$$\mathbf{J}^b = \mu_0^{-1}[\chi_n(\mathbf{B}\cdot\hat{\mathbf{n}})\hat{\mathbf{n}} + \chi_m(\mathbf{B}\cdot\hat{\mathbf{m}})\hat{\mathbf{m}} + \chi_l(\mathbf{B}\cdot\hat{\mathbf{l}})\hat{\mathbf{l}}], \tag{IX.2}$$

where μ_0 is the permeability of free space. The corresponding magnetic free-energy density is given by

$$g_\chi = -\int_0^{\mathbf{B}} \mathbf{J}^b\cdot d\mathbf{B} = -\frac{1}{2\mu_0}[\chi_n(\mathbf{B}\cdot\hat{\mathbf{n}})^2 + \chi_m(\mathbf{B}\cdot\hat{\mathbf{m}})^2 + \chi_l(\mathbf{B}\cdot\hat{\mathbf{l}})^2]. \tag{IX.3}$$

In the same way one can derive an expression for the electric free-energy density

$$g_\varepsilon = -\frac{\varepsilon_0}{2}[\varepsilon_n(\mathbf{E}\cdot\hat{\mathbf{n}})^2 + \varepsilon_m(\mathbf{E}\cdot\hat{\mathbf{m}})^2 + \varepsilon_l(\mathbf{E}\cdot\hat{\mathbf{l}})^2] \tag{IX.4}$$

where we have introduced ε_0, the permittivity of free space.

Let us start to investigate the effect of applying a magnetic field in the z-direction,

$\mathbf{B} = B\hat{\mathbf{z}}$, employing the coordinates of Figure 2. Substituting the three unit vectors $\hat{\mathbf{n}}$, $\hat{\mathbf{m}}$ and $\hat{\mathbf{l}}$ as given by Equation (IV.1)–(IV.3) into Equation (IX.3), the magnetic free-energy density is given by

$$g_\chi = -\frac{B^2}{2\mu_0}[\chi_n\cos^2\theta + (\chi_m\sin^2\psi + \chi_l\cos^2\psi)\sin^2\theta]. \tag{IX.5}$$

Minimizing g_χ with respect to θ and ψ gives the conditions

$$[\chi_n - (\chi_m\sin^2\psi + \chi_l\cos^2\psi)]\sin 2\theta = 0, \tag{IX.6}$$

$$(\chi_l - \chi_m)\sin 2\psi \sin^2\theta = 0. \tag{IX.7}$$

Equations (IX.6) and (IX.7) have three solutions which are shown in Figure 9. In order to determine which of these is the stable one, we have to compare the magnetic free-energy density of the system for the three cases. The three solutions are:

Solution I

$$\theta = 0, \quad \psi \text{ undetermined}; \qquad g_\chi = -\frac{B^2}{2\mu_0}\chi_n.$$

Here $\hat{\mathbf{n}}$ is parallel to $\mathbf{B}$, while the m-director is free to point in any direction perpendicular to $\mathbf{B}$.

Solution II

$$\theta = \pi/2, \quad \phi \text{ undetermined}, \qquad \psi = \pi/2; \qquad g_\chi = -\frac{B^2}{2\mu_0}\chi_m,$$

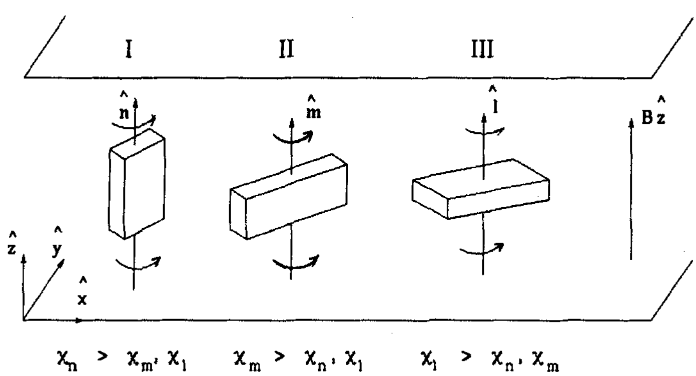

FIGURE 9 Ordering of a biaxial plate in the presence of a magnetic field. The axis of the biaxial plate corresponding to the largest value of χ_i points in the direction of the field, while the other two axes are free to rotate in any compatible directions perpendicular to the field.

Here $\hat{\mathbf{m}}$ is parallel to **B**, while the n-director is free to point in any direction perpendicular to **B**.

Solution III

$$\theta = \pi/2, \quad \phi \text{ undetermined}, \qquad \psi = 0; \qquad g_X = -\frac{B^2}{2\mu_0}\chi_l.$$

Here $\hat{\mathbf{l}}$ is parallel to **B**, while the n- and the m-directors are free to point in any compatible directions perpendicular to **B**.

Which of the three solutions is stable is determined by that which minimizes the free-energy density. Thus we find that the axis corresponding to the largest magnetic susceptibility points in the direction of the field, while the system adopts the same magnetic energy for each possible direction of the other two axes, now being perpendicular to the field, and thus the direction of these two axes is undetermined by the field. As is seen from Equations (IX.3) and (IX.4), if we instead want to study the influence of an electric field we only have to make the substitution $B^2\chi_i/\mu_0 \rightarrow \varepsilon_0 E^2 \varepsilon_i$.

As we saw above, applying an electric or a magnetic field across a biaxial nematic system is not enough to order the system completely. Chandrasekhar has suggested[19] that applying a magnetic and an electric field at right angles to each other could be one way to orient both directors unambiguously. However, it turns out that the analysis of the effect of two crossed electric and magnetic fields over a biaxial nematic in the general case is a rather involved problem and this is discussed in detail elsewhere.[20] Here we restrict ourselves to a discussion of the case for which the electric field is much stronger than the magnetic one, i.e., to the case $\varepsilon_0 E^2 \gg \mu_0^{-1} B^2$. Below it is proved that in this case the axis corresponding to the largest ε_i is ordered by the electric field, while the magnetic field aligns the one of the two remaining axes that has the largest χ_i. That this happens is not obvious, because one could expect the axes to be oriented at some oblique angles with respect to the fields due to the competition from the electric and magnetic torques. Before proceeding we introduce a notation that incorporates the coupling constants of the fields into the susceptibilities

$$\tilde{\varepsilon}_i = \varepsilon_0 E^2 \varepsilon_i, \qquad \tilde{\varepsilon}_{ij} = \varepsilon_0 E^2 \varepsilon_{ij},$$

$$\tilde{\chi}_i = \mu_0^{-1} B^2 \chi_i, \qquad \tilde{\chi}_{ij} = \mu_0^{-1} B^2 \chi_{ij}. \tag{IX.8}$$

Assuming that the electric field is much stronger than the magnetic one, it can generally be stated

$$\tilde{\varepsilon}_i \gg \tilde{\chi}_j, \qquad \tilde{\varepsilon}_{ij} \gg \tilde{\chi}_{kp}, \tag{IX.9}$$

for all i, j, k and p. To analyse the situation it is most convenient in this case to express the torque components in their Cartesian form. Generally, the magnetic torque can be written as $\mathbf{\Gamma}^{\chi} = \mathbf{J}^{b} \times \mathbf{B}$, while a similar expression is valid for the electric torque. Using tensorial notation, the electro-magnetic torque is instead given by Equations (II.5)–(II.7). Assuming that the fields are given by $\mathbf{E} = E\hat{\mathbf{x}}$ and $\mathbf{B} = B\hat{\mathbf{z}}$, respectively, the electro-magnetic torque is given by

$$\Gamma_x^{\chi\varepsilon} = \tilde{\chi}_{nl} n_y n_z + \tilde{\chi}_{ml} m_y m_z,$$

$$\Gamma_y^{\chi\varepsilon} = -\tilde{\chi}_{nl} n_x n_z - \tilde{\chi}_{ml} m_x m_z + \tilde{\varepsilon}_{nl} n_x n_z + \tilde{\varepsilon}_{ml} m_x m_z,$$

$$\Gamma_z^{\chi\varepsilon} = -\tilde{\varepsilon}_{nl} n_x n_y - \tilde{\varepsilon}_{ml} m_x m_y. \tag{IX.10}$$

From Equations (IX.10) one sees immediately that all configurations for which two of the three vectors $\hat{\mathbf{n}}$, $\hat{\mathbf{m}}$ and $\hat{\mathbf{l}}$ are parallel to the fields are possible equilibrium configurations of the system. Figure 10 shows these solutions and also gives the appropriate conditions for each of these to be stable. In the figure we have also

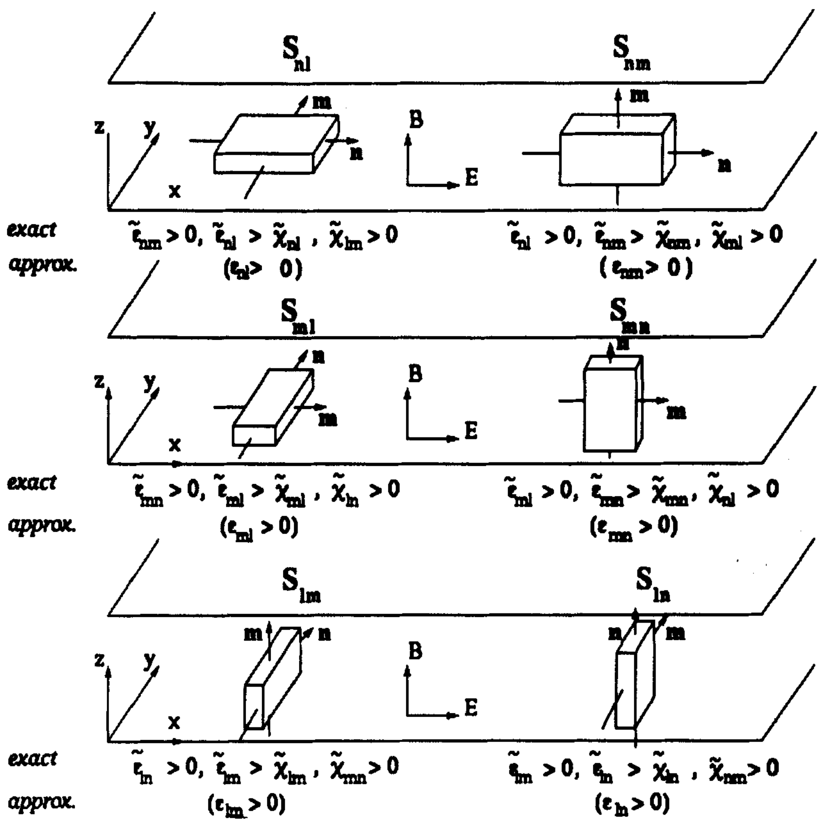

FIGURE 10 The six equilibrium configurations of biaxial nematics in the presence of two perpendicular electric and magnetic fields. The condition for each solution to be stable is also displayed in the figure. In the case when the electric field is much stronger than the magnetic one, the second condition in each set can be replaced by an approximate one according to the figure. In the figure we also introduce a shorthand notation for the equilibrium configurations.

introduced a shorthand notation for these configurations in such a way that the solution S_{ij} corresponds to the situation for which the i director is pointing in the direction of the electric field and the j director is pointing in the direction of the magnetic field.

In order to investigate the stability of the solutions we have to determine the torque acting on the directors when the system is allowed to perform small perturbations around these solutions. Let us study the solution characterized by $\hat{\mathbf{n}} = \hat{\mathbf{x}}$ and $\hat{\mathbf{m}} = \hat{\mathbf{y}}$. A small perturbation of this configuration can be expressed by three infinitesimal rotations α, β and γ around the coordinate axes, respectively. If α, β and γ are small, the perturbed directors are given by

$$n_x \approx 1, \qquad n_y \approx \gamma, \qquad n_z \approx -\beta, \tag{IX.11}$$

and

$$m_x \approx -\gamma, \qquad m_y \approx 1, \qquad m_z \approx \alpha. \tag{IX.12}$$

The torque $\Gamma^{pert.}$ acting on the director is now derived from Equations (IX.10)–(IX.12)

$$\Gamma_x^{pert.} \approx \tilde{\chi}_{ml}\alpha, \qquad \Gamma_y^{pert.} \approx (\tilde{\chi}_{nl} - \tilde{\varepsilon}_{nl})\beta, \qquad \Gamma_z^{pert.} \approx \tilde{\varepsilon}_{mn}\gamma. \tag{IX.13}$$

If the solution is stable, the torque (IX.13) must be such that it acts to bring the directors back to the unperturbed solution, i.e., all the three components of $\Gamma^{pert.}$ must be negative. We thus derive the following conditions for stability

$$\tilde{\varepsilon}_{nm} > 0, \qquad \tilde{\varepsilon}_{nl} > \tilde{\chi}_{nl}, \qquad \tilde{\chi}_{lm} > 0. \tag{IX.14}$$

With the assumption that the electric field is much stronger than the magnetic one this can be approximated by

$$\varepsilon_{nm} > 0, \qquad \varepsilon_{nl} > 0, \qquad \chi_{lm} > 0. \tag{IX.15}$$

By analysing the remaining five solutions in the same way, one derives the equilibrium conditions for stability that are given in Figure 10. In the case when $\varepsilon_0 E^2 >> \mu_0^{-1} B^2$, the result of the stability analysis is that the axis with the largest ε_i falls along the electric field, while the one of the two remaining axes with the largest χ_i falls along the magnetic field.

The result stated above is fairly obvious once we have convinced ourselves that the equilibrium solutions will correspond to these orientations for which the directors fall along the axes of the coordinate system. However, we must emphasize that the conditions of the type (IX.15) are only valid in the case $\varepsilon_0 E^2 >> \mu_0^{-1} B^2$ or, of course, with obvious changes when $\mu_0^{-1} B^2 >> \varepsilon_0 E^2$. In the case when the two fields are of competing order of magnitude, the general stability criteria displayed in Figure 10 must be considered, and in this case the behaviour of the system is much more complex to analyse, and in some cases even bistability is exhibited. A full treatment of this problem is, however, discussed elsewhere.[20]

X THE EFFECTIVE VISCOSITIES

The stress tensor defined by Equation (II.8) introduces fifteen viscosity coefficients into the dynamic theory of biaxial nematics, although three Onsager relations (Equations (II.11)) reduce the number of independent viscosity coefficients to twelve. In order to measure these it is necessary to perform twelve independent measurements, each of which determines some combination of the viscosity coefficients linearly independent of the others. In Section VI we defined three rotational viscosities which are given by Equations (VI.11). Below we show that it is possible to define nine effective shearing viscosities which are linearly independent of each other. Thus one can design sufficient experiments to determine the full set of viscosity coefficients needed to give a complete description of the system.

To calculate the effective viscosities of the system, we use the equations of Section II. Assuming a shear flow of the type shown in Figures 6 and 7, i.e., assuming a velocity profile $\mathbf{v} = v(z)\hat{\mathbf{x}}$, Equation (II.3) reduces to

$$t_{xz,z} = 0, \tag{X.1}$$

which can be integrated to read

$$t_{xz} = \tau, \tag{X.2}$$

where the integration constant τ represents the force per unit area applied to the moving plate. The xz-component of the viscous stress tensor, being a function of the directors, can generally be written as

$$t_{xz} = v'g(n_i, m_j). \tag{X.3}$$

Equations (X.2) and (X.3) give

$$g(n_i, m_j) = \frac{\tau}{v'}, \tag{X.4}$$

i.e., $g(n_i, m_j)$, being the ratio of the driving force and the corresponding shear rate, can be interpreted as the viscosity function of the system. By the use of Equations (II.8) and (X.4) we can write this as

$$\begin{aligned} g = \frac{1}{2}[&2\alpha_1 n_x^2 n_z^2 - \alpha_2 n_z^2 + \alpha_3 n_x^2 + \alpha_4 + \alpha_5 n_z^2 + \alpha_6 n_x^2 \\ &+ 2\beta_1 m_x^2 m_z^2 - \beta_2 m_z^2 + \beta_3 m_x^2 + \beta_5 m_z^2 + \beta_6 m_x^2 \\ &+ \mu_1(n_x m_z - n_z m_x) n_z m_x + \mu_2(n_x m_z - n_z m_x) n_x m_z \\ &+ \mu_3(n_x m_z + n_z m_x) n_z m_x + \mu_4(n_x m_z + n_z m_x) n_x m_z]. \end{aligned} \tag{X.5}$$

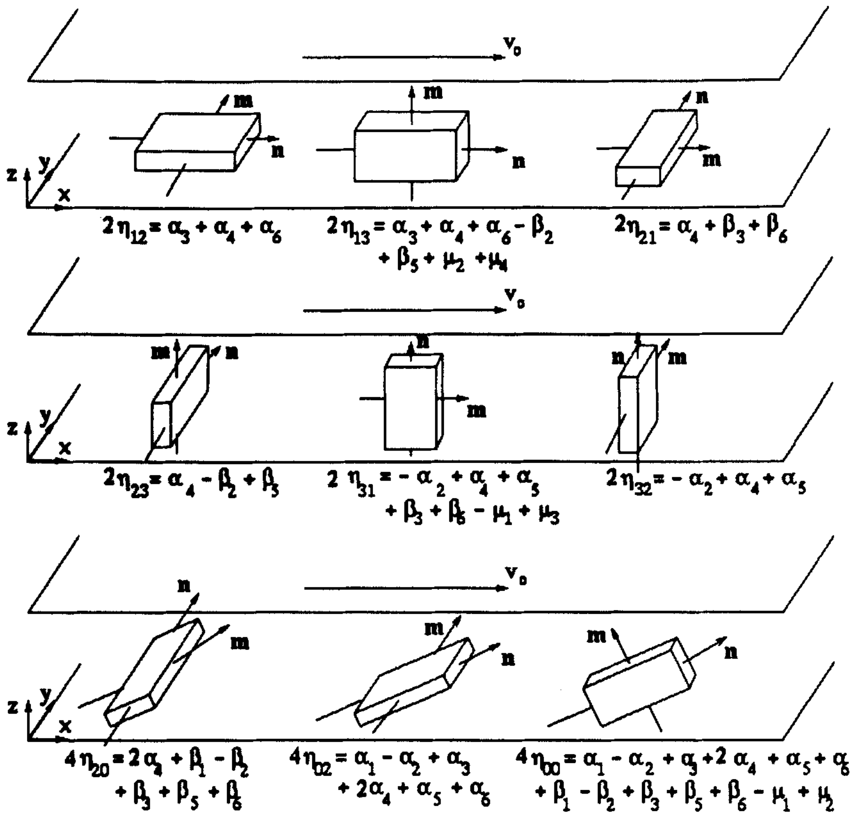

FIGURE 11 The nine linearly independent effective viscosities of biaxial nematics which we chose to define.

As shown in Section IX, it is possible to order the directors by a suitable arrangement of crossed electric and magnetic fields. If these fields are strong enough, the corresponding torque is sufficient to dominate the shearing torque introduced by the flow, and we thus have a means to control the directors in the presence of a flow. Figure 11 shows the nine different orientations of the directors corresponding to the nine linearly independent effective viscosities which we chose to define. These are the six orientations for which the directors are parallel to the coordinate axes, and three oblique orientations, where either one or both of the directors make a forty five degree angle with the x-axis. We introduce a notation η_{ij} for these viscosities in the following way. Denote the first index 1, 2, or 3, depending upon whether the n-director is pointing in the x, y or z-direction, and in the same way let the second index define the direction of the m-director. In the case for which one or both of the directors are pointing in one of the oblique directions we instead denote the corresponding index by 0. As the flow must always be in the same direction as the driving force, one concludes that each of the effective viscosities must be positive. To summarize we have thus defined the following effective viscosities

$$\eta_{12} = \frac{1}{2}(\alpha_3 + \alpha_4 + \alpha_6) > 0,$$

$$\eta_{13} = \frac{1}{2}(\alpha_3 + \alpha_4 + \alpha_6 - \beta_2 + \beta_5 + \mu_2 + \mu_4) > 0,$$

$$\eta_{21} = \frac{1}{2}(\alpha_4 + \beta_3 + \beta_6) > 0,$$

$$\eta_{23} = \frac{1}{2}(\alpha_4 - \beta_2 + \beta_5) > 0,$$

$$\eta_{31} = \frac{1}{2}(-\alpha_2 + \alpha_4 + \alpha_5 + \beta_3 + \beta_6 - \mu_1 + \mu_3) > 0,$$

$$\eta_{32} = \frac{1}{2}(-\alpha_2 + \alpha_4 + \alpha_5) > 0,$$

$$\eta_{20} = \frac{1}{4}(2\alpha_4 + \beta_1 - \beta_2 + \beta_3 + \beta_5 + \beta_6) = \frac{1}{4}(2\eta_{21} + 2\eta_{23} + \beta_1) > 0,$$

$$\eta_{02} = \frac{1}{4}(\alpha_1 - \alpha_2 + \alpha_3 + 2\alpha_4 + \alpha_5 + \alpha_6) = \frac{1}{4}(2\eta_{12} + 2\eta_{32} + \alpha_1) > 0,$$

$$\begin{aligned}\eta_{00} &= \frac{1}{4}(\alpha_1 - \alpha_2 + \alpha_3 + 2\alpha_4 + \alpha_5 + \alpha_6 \\ &\quad + \beta_1 - \beta_2 + \beta_3 + \beta_5 + \beta_6 - \mu_1 + \mu_2) \\ &= \frac{1}{4}(2\eta_{13} + 2\eta_{31} + \alpha_1 + \beta_1 - \mu_3 - \mu_4) > 0, \end{aligned} \tag{X.6}$$

where the corresponding orientations of the directors are shown in Figure 11.

In conclusion: The stress tensor (II.8) introduces fifteen viscosity coefficients related by the three Onsager relations (II.11). To measure these, one must measure the three rotational viscosities (Figure 4) given by Equations (VI.11) and the nine effective shearing viscosities (Figure 11) given by Equations (X.6).

XI TRANSVERSE FLOW EFFECTS

It is well known from the study of uniaxial nematics[21] that under some circumstances a transverse flow can be induced in the system. Such a transverse flow could be used to design additional experiments to determine some viscosity coefficients of the system. However, what is more important is that for some configurations of the flow, transverse flow is inevitable and an analysis of the problem neglecting transverse flow might prove to be incorrect. In order to assure ourselves that the results derived in the previous sections do not suffer from such an oversight, we give a brief study of shear flow incorporating the possibility of transverse flow into the equations.

Performing a shear flow experiment in the geometry of Figure 2 and allowing for transverse flow, one must consider a velocity field $\mathbf{v}(z)$ of the form

$$v_x = v(z), \qquad v_y = u(z), \qquad v_z = 0. \tag{XI.1}$$

The x- and y-components of the equation (II.3) can in the absence of external body forces be written

$$t_{xz,z} = 0, \qquad t_{yz,z} = 0, \tag{XI.2}$$

and by integrating these equations, assuming the driving force $\boldsymbol{\tau}$ to be applied in the x-direction, i.e., $\boldsymbol{\tau} = \tau\hat{\mathbf{x}}$, one obtains

$$t_{xz} = \tau, \qquad t_{yz} = 0. \tag{XI.3}$$

Again assuming $\dot{n}_i = \dot{m}_i = 0$, the quantities defined by Equations (II.9) and (II.10) now include additional terms proportional to the transverse shear rate u' where

$$u' = \frac{dv_y}{dz}. \tag{XI.4}$$

Substituting these more general expressions into the stress tensor (II.8), one derives

$$t_{yz} = \frac{1}{2}[v'X + u'Y], \tag{XI.5}$$

where we have introduced X and Y according to

$$\begin{aligned} X = {} & 2\alpha_1 n_x n_y n_z^2 + \alpha_3 n_x n_y + \alpha_6 n_x n_y \\ & + 2\beta_1 m_x m_y m_z^2 + \beta_3 m_x m_y + \beta_6 m_x m_y \\ & + (n_x m_z - n_z m_x)(\mu_1 m_y n_z + \mu_2 n_y m_z) \\ & + (n_x m_z + n_z m_x)(\mu_3 m_y n_z + \mu_4 n_y m_z), \end{aligned} \tag{XI.6}$$

$$
\begin{aligned}
Y = {} & 2\alpha_1 n_y^2 n_z^2 - \alpha_2 n_z^2 + \alpha_3 n_y^2 + \alpha_4 + \alpha_5 n_z^2 + \alpha_6 n_y^2 \\
& + 2\beta_1 m_y^2 m_z^2 - \beta_2 m_z^2 + \beta_3 m_y^2 + \beta_5 m_z^2 + \beta_6 m_y^2 \\
& + (n_y m_z - n_z m_y)(\mu_1 m_y n_z + \mu_2 n_y m_z) \\
& + (n_y m_z + n_z m_y)(\mu_3 m_y n_z + \mu_4 n_y m_z). \qquad \text{(X1.7)}
\end{aligned}
$$

The second of Equations (XI.3) together with Equation (XI.5) implies

$$u' = -v' \frac{X}{Y}. \qquad \text{(XI.8)}$$

Thus the possibility of inducing a transverse flow occurs whenever $X \neq 0$.

From the structure of X one notices that transverse flow effects are possible when either of the two directors is pointing out of the shear plane, but not parallel to the y-direction. All the geometrical configurations discussed previously in this paper are of such a nature that the directors have either been confined within the shear plane or are parallel to the y-axis. Thus we conclude that transverse flow effects do not influence the analysis of the situations presented in this paper.

XII DISCUSSION

In this paper, we have discussed the flow properties of the biaxial nematic phase with the stress tensor (II.8) derived in Section II as a starting point. In order to construct a physical model of the system, we introduced the biaxial plate in Figure 1*b*, and our interest in a biaxial system of "rod-like" symmetry led us to introduce the notations long director $\hat{\mathbf{n}}$ and transverse director $\hat{\mathbf{m}}$ according to the figure. Our aim throughout the paper has been to show how much the flow behaviour of the biaxial nematic phase is similar to the corresponding behaviour of uniaxial nematics. For example, in shear flow, with one of the two directors pointing in the isotropic or perpendicular direction, the mathematical structure of the governing equations exactly resembles that of the uniaxial nematic phase with one set of viscosity coefficients α_i corresponding to the long director and another set β_i corresponding to the transverse director. A complication in the study of biaxial nematics is the presence of the coupling constants μ_i which appear in the general case when neither of the two directors is pointing in the isotropic direction.

Presently, no experimental information regarding the viscosity coefficients of biaxial nematics exists. However, we have argued that it seems reasonable to assume that one can use the knowledge of the Leslie coefficients of uniaxial nematics to estimate the values for some of the corresponding coefficients of biaxial nematics. Such an assumption, together with the inequalities derived in Section VI, leads to the viscosity coefficients of the system displayed in Table I.

In connection with Figure 4, we have shown how one can introduce three rotational viscosities of the biaxial nematic phase, each of which corresponds to a rotation of the biaxial plate around one of its three principal axes. We have also shown (Figure 5) that in the general case, the rotational motion of the system is accompanied by a transverse torque, which probably is important when analyzing the route towards equilibrium for the directors.

In the presence of shear flow the system exhibits six possible equilibrium orientations occurring in pairs (Figure 7). Depending on the values of the viscosity coefficients, any of these pairs may or may not exist independently. To understand the nature of the stability of these equilibrium angles in terms of the viscosity coefficients is a rather complex procedure. We have given a few different examples of stability in Table II, showing that any of the three solutions that we have denoted **FP**, **FB** and **PF** can be stable for certain combinations of the viscosity coefficients. Studying Figure 7, one again appreciates the similarity with the case of flow alignment for uniaxial nematics.

By applying two crossed electric and magnetic fields over the system it is possible to orient the directors under certain circumstances. In Figure 10, we show the six possible equilibrium configurations which are possible in this case, and also give the proper conditions for stability for each of these. The general analysis of these stability conditions has been discussed elsewhere[20] where it is shown that in some cases the system can exhibit bistability. Thus the experimentalist must approach the problem of aligning the system by using electric and magnetic fields with some caution.

Having aligned the system in a proper way, one can define nine effective shearing viscosities shown in Figure 11. Measuring these together with the three rotational viscosities makes it possible to determine the full set of viscosity coefficients of the system. However the experimental difficulties in performing such a measurement are probably extensive.

To summarize, we conclude that the biaxial nematic phase provides a fascinating system, the flow properties of which exhibit large similarities to the uniaxial nematic system. However, the general behaviour is more complex and provides many effects due to the coupling between the two directors that are not present in uniaxial nematics. Thus we predict that it will probably demand a great deal of effort before the behaviour of biaxial nematics has been investigated and understood to a reasonable degree. Our hope is that this paper will prove a useful guide to those who are interested in undertaking such a task.

References

1. L. J. Yu and A. Saupe, *Phys. Rev. Lett.*, **45**, 1000 (1980).
2. J. Malthête, L. Liebert, A. M. Levelut and Y. Galerme, *C. R. Acad. Sci. Paris*, **303**, 1073 (1986).
3. S. Chandrasekhar, B. K. Sadashiva, B. R. Ratna and V. N. Raja, *Pramana*, **30**, L491 (1988).
4. K. Praeffke, B. Kohne, B. Gundogan, D. Demus and S. Diele, 18. Arbeitstagung Flussigkristalle (1989).
5. A. Saupe, *J. Chem. Phys.*, **75**, 5118 (1981).
6. H. Brandt and H. Pleiner, *Phys. Rev.*, **A24**, 2777 (1981).
7. U. D. Kini, *Mol. Cryst. Liq. Cryst.*, **108**, 71 (1984).
8. E. Govers and G. Vertogen, *Physica*, **133A**, 337 (1985).
9. D. Baals, *Z. Naturforsch.*, **45A**, 7 (1990).
10. J. L. Ericksen, *Trans. Soc. Rheol.*, **5**, 23 (1961).

11. F. M. Leslie, *Arch. Rat. Mech. Anal.*, **28**, 265 (1968).
12. J. S. Laverty and F. M. Leslie, "*Proc. Third European Rheology Conference*" (ed. D. R. Oliver), Elsevier Applied Science (London and New York 1990), pp. 310–312.
13. E. Govers and G. Vertogen, *Phys. Rev.*, **A30**, 1998 (1984).
14. T. Carlsson, *Phys. Rev.*, **A34**, 3393 (1986).
15. H. Kneppe, F. Schneider and N. K. Sharma, *J. Chem. Phys.*, **77**, 3203 (1982).
16. H. Kneppe, F. Schneider and N. K. Sharma, *Ber. Bunsenges. Phys. Chem.*, **85**, 784 (1981).
17. T. Carlsson, F. M. Leslie and J. S. Laverty, to be published.
18. L. Meirovitch, "*Elements of Vibrational Analysis*" McGraw-Hill, 1975.
19. S. Chandrasekhar, Paper presented at *8th Liquid Crystal Conference of Socialist Countries*, Krakow, Poland, August 1989.
20. T. Carlsson and F. M. Leslie, *Liq. Cryst.*, **10**, 325 (1991).
21. P. Pieranski and E. Guyon, *Phys. Lett.*, **49A**, 237 (1974).